On the phase transition in benzil

A. Yoshihara, W. D. Wilber, E. R. Bernstein, and J. C. Raich

On the phase transition in benzil[a)]

A. Yoshihara, W. D. Wilber, E. R. Bernstein, and J. C. Raich

Departments of Physics and Chemistry, Colorado State University, Fort Collins, Colorado 80523

The phase transition in crystalline benzil $[(C_6H_5CO)_2]$ at 84 K is investigated through Brillouin scattering. The major experimental findings are two transverse acoustic phonon modes exhibiting softening near the phase transition, a longitudinal acoustic mode that is temperature sensitive, and the ratio of the Rayleigh peak intensity to the soft mode intensity behaves anomalously. These results are discussed using a theory developed for an elastic phase transition in *sym*-triazine $(C_3N_3H_3)$. It is found that bilinear-coupling terms involving strains and the order parameter can explain transverse mode behavior but not that of the longitudinal acoustic mode.

I. INTRODUCTION

Benzil $(C_6H_5CO)_2$ is a molecular crystal which has a crystallographic phase transition at ~ 84 K. Since the discovery of this phase transition through birefringence studies,[1] many experimental techniques have been employed to investigate this system. The phase transition has been characterized using EPR spectroscopy,[2] x-ray diffraction,[3] specific heat measurements,[4] infrared spectroscopy,[5] Raman scattering,[6] and Brillouin scattering.[7] The high temperature phase has been determined to possess a trigonal structure $D_3^4(P3_121)$ with 3 molecules/unit cell. The structure of the low temperature phase is assigned as $C2$.[8] The benzil molecule has a permanent dipole moment of 3.58 D.[9] The crystal contains planar arrays of benzil molecules, the twofold axes of which coincide with the twofold axes of these arrays, with each succeeding plane related to the one below it by a threefold screw axis.[10] The dipole moments of a given layer are all aligned in the same direction in the plane of the layer. The aligned dipole moments are related to those in other layers by the threefold screw axis and no spontaneous polarization appears in the high temperature phase. In the low temperature phase the threefold symmetry axis is lost and a spontaneous polarization results. Benzil, however, is different from most ferroelectrics in that the spontaneous polarization (P_s) cannot be reversed by an external electric field: in a given domain, P_s and $-P_s$ are not equivalent. Therefore, benzil is considered an example of a pyroelectric.

A Raman scattering study[6] characterized a soft E mode which splits in the low temperature phase. The dielectric constant ϵ_a shows a weak Curie–Weiss-like anomaly near T_c $[\Delta\epsilon_a(T_c)/\epsilon(300 \text{ K}) \sim 0.5\%]$. Spontaneous polarization[8] (~ 0.1 μC/cm^2) appears along the a_m axis (twofold axis) below the transition temperature.

Although the dielectric anomaly is weak, recent Brillouin scattering results reveal two soft transverse acoustic phonons which propagate along the a and c axes. The transverse mode along the a axis displays a faster softening than the c-axis mode. These phonons belong to the E irreducible representation of D_3. The elastic constant c_{11} which is obtained from the frequency

shift of a longitudinal phonon propagating along the a axis also shows some softening in the neighborhood of the transition temperature. Anisotropies in "slowness" $(v^{-1}; v =$ sound velocity) are also predicted in both the $a-c$ and $b-c$ planes. Softening in the $a-b$ plane is, however, fairly uniform.

The above experimental results suggest that the order parameter for this phase transition is some physical quantity which belongs to the E irreducible representation of D_3. This representation contains as basis functions polarizations (P_x, P_y), strains (e_4, e_5), $(e_6, e_7 = e_1 - e_2)$, and molecular rotations (R_x, R_y). Observed anomalies in dielectric and elastic properties are consequences of bilinear coupling between some microscopic order parameter and such macroscopic quantities as strains and polarizations.

The transition is expected to be first order based on the Landau condition for third-order invariants $[E]^3$ in the free energy expansion. Although theory predicts a first-order transition, experiments reveal only a weakly first-order transition at $T = T_c$; the latent heat[4] associated with the transition is quite small $(\Delta H \sim 44$ J mol$^{-1})$ and the hysteresis is smaller than 0.1 K.[3,6]

Recently, Raich and Bernstein[11] have developed a description of the ferroelastic phase transition in *sym*-triazine $(T_c \sim 200$ K). The phase transition is induced by a doubly degenerate order parameter which belongs to the E_g irreducible representation of D_{3d}. The low temperature phase, in this case, has C_{2h} symmetry. The elastic constant c_{44} is predicted to soften at this phase transition, in agreement with recent inelastic neutron scattering experiments.[12]

As benzil is piezoelectric, even in the high temperature phase dielectric and elastic anomalies cannot be separated, in general. The observed elastic constants must be described by[13]

$$c_{ij} = c_{ij}^0 - a_{ijk}^2 \epsilon_k \ ,$$

in which c_{ij}^0 is a bare elastic constant, a_{ijk} is a piezoelastic constant, and ϵ_k is a bare dielectric constant. The dielectric constant can be decomposed to a sum of two terms: $\epsilon_k = \epsilon_k^0 + \Delta\epsilon_k$ in which ϵ_k^0 is the normal part and $\Delta\epsilon_k$ represents the anomalous part of the dielectric constant. For benzil, $\epsilon_k^0 \gg \Delta\epsilon_k$ for all temperatures. Therefore, the main effect of the piezoelectric property

of benzil is to shift the absolute values of the elastic constants. Ignoring this piezoelectric coupling effect, interactions between order parameters and strains can be separated from interactions between order parameters and polarizations. Moreover, since elastic constant matrices for D_3 and D_{3d} are the same, the elastic anomalies in benzil can be treated in this regime by the theoretical model developed for sym-triazine.[11]

In this report, new Brillouin scattering data for phonons propagating along the a and c axes will be presented. We became aware of the previous Brillouin results[7] only after our experiments were nearing completion. Our results are in substantial agreement with those of Ref. 7 but extend the data for the longitudinal modes, in particular. The observed temperature behavior is discussed on the basis of a Landau mean field theory worked out for triazine, which undergoes a similar transition, on the basis of group theory. Deviations from the Landau theory are noted and discussed qualitatively in terms of different mechanisms.

II. EXPERIMENTAL

Single crystals of benzil were grown from xylene solutions by slow cooling or slow evaporation. Solutions are prepared by successive and repeated recrystallizations and filterings of benzil and xylene. Large single transparent, pale yellow crystals ($\sim 2 \times 5 \times 1$ cm^3) of excellent optical quality are readily grown. Crystal axes are determined by examining the crystal with a polarizing microscope and observing the crystal's external features.[6,14] Since the crystal is brittle, samples for 90° scattering in the a-c plane were carefully cut and then polished using lens paper and xylene solvent to obtain cubic samples about 5 mm on a side. In order to measure anisotropy of frequency shifts in the a-c plane, several cylindrically shaped samples were prepared (~ 8 mm diam$\times 10$ mm). To reduce surface scattering, samples were coated with a thin layer of parafin oil. This procedure drastically reduced the Rayleigh intensity ($\sim 1/10$).

The experimental setup is such that Brillouin scattering and correlation spectroscopy can be simultaneously observed by splitting the scattered light. Details of the correlation spectroscopy apparatus and results will be presented at a later time. Brillouin spectra were obtained using a piezoelectrically scanned triple pass Fabry–Perot interferometer followed by an RCA C31034A-02 photomultiplier tube thermoelectrically cooled for a dark count of ~ 10 cps. The output of the tube is detected by photon counting electronics and a data acquisition and stabilization system (Burleigh DAS-1). Spectra are stored in a Nicolet 1074 multichannel analyzer and displayed on a Hewlett–Packard 9845S computer or an x-y recorder. Free spectral ranges of 28.68 and 10.0 GHz are typical. A finesse of ~ 50 to 60 could be maintained for the duration of the experiment (~ 1 to 2 days).

The laser employed is a Spectra Physics Model 165 argon ion laser. Typical power at the sample was ~ 100 mW at 5145 Å. An intracavity etalon provided
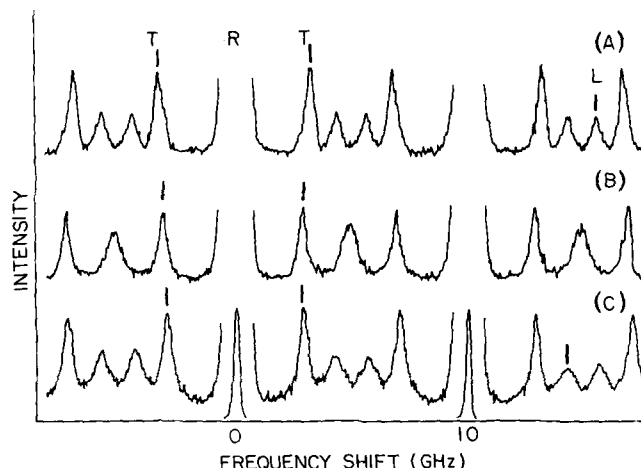

FIG. 1. Brillouin spectra of phonons propagating along the a axis near the transition temperature in the high temperature phase: (A) $T_c + 1.5$ K, (B) $T_c + 0.5$ K, (C) $\sim T_c$, in which $T_c = 81.5$ K for this particular heavily recycled sample. Brillouin peaks corresponding to a Rayleigh peak which is denoted by "R" are labeled "T" and "L" with vertical line markers.

single mode output, which is monitored with a spherical Fabry–Perot interferometer used as a spectrum analyzer. Samples are affixed to a copper block, using G. E. 7031 varnish, and then placed in a copper scattering cell wrapped with heater wire. A closed cycle refrigerator (CTI 21) is used to obtain temperatures as low as 40 K. Temperature is controlled with a proportional controller with a diode sensor to within ± 0.1 K. Sample temperature is measured with another diode through the controller. Transition temperature for each sample is found to be 83.5 K± 0.5 K. Experimental errors are estimated as follows: crystal orientation (phonon propagation direction) is $\pm 2°$, Brillouin shift measurements are $\pm 0.5\%$ for L modes and $\pm 1\%$ for T modes, half width of transitions is $\pm 5\%$, and intensity measurements are $\pm 15\%$.

III. RESULTS

Typical temperature dependent phonon frequencies near the transition temperature are shown in Fig. 1 for phonons propagating along the a axis. Although no physical damage was visible in the sample after several cycles through the transition temperature, softening of the transverse modes became less pronounced and the transition temperature decreased (as can be seen in Fig. 1). The longitudinal phonon evidences rapid changes in the region near T_c. The other transverse phonon is masked by the soft mode in the region displayed in Fig. 1. Results for the a- and c-axis phonons in the high temperature phase correspond closely to the previous Brillouin scattering results[7]; note however, that the frequencies reported here are slightly ($\sim 3\%$) higher. Temperature dependence for the longitudinal a-axis phonon frequency and its half width at half maximum are given in Fig. 2. The frequency shift of L_a with temperature shows a λ-type anomaly in addition to a discontinuity at T_c, and its half width increases con-
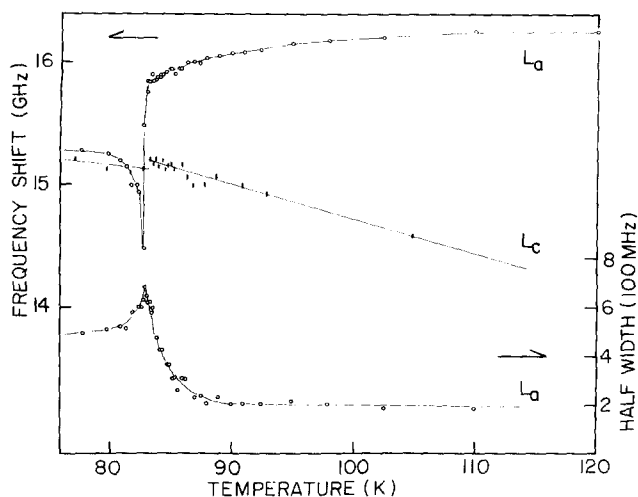
FIG. 2. Temperature dependence of the frequency shift and HWHM of the LA phonon along the a axis (L_a) and the frequency shift of the LA phonon along the c axis (L_c). Slight differences can be seen for different samples. The lines are drawn to help view the overall trends.

siderably near the transition temperature. The longitudinal c-axis phonon evidences no anomaly in frequency shift or half width; it displays a monotonic variation with temperature. These data are also presented in Fig. 2.

Two transverse modes propagating along the a axis are observed, as is to be expected for a trigonal structure.[15] The less intense of the two shows a weak temperature dependence. Along the c axis only one transverse mode is found; it is doubly degenerate and soft.

Results for the transverse soft modes are summarizer in Fig. 3. The a-axis phonon is always of lower frequency than the c-axis phonon; the a-axis mode shows a small jump at T_c and has a small ($\lesssim 1$ K) transition temperature hysteresis. These facts suggest that the phase transition is of first order. Measurements have been repeated using different samples cut from the same crystal boule, and a weak sample dependence has been observed in the soft mode behavior near the transition temperature (see Fig. 3). For a given sample, however, good reproducibility was observed. The slight sample dependent frequency data can probably be ascribed to defects which create variation in the local stress distribution in the samples.

The ratio of the soft mode intensity to Rayleigh peak intensity along the a axis was also measured and is summarized in Fig. 3. Initial increase of this ratio is due to soft mode behavior, i.e., $I_B \propto (\rho v^2)^{-1}$ [15] and $v \to 0$. The ratio has a maximum at $\sim T_c + 1$ K, however, suggesting, in addition, a rapid increase in Rayleigh intensity in the high temperature phase close to the transition temperature.

Sound velocity v can be caluclated for an optically anisotropic crystal[16] by

$$\omega_B = \frac{2\pi'}{\lambda} v (n_i^2 + n_s^2 - 2n_i n_s \cos\theta_s)^{1/2} ,$$

in which n_i, n_s are refractive indices for incident and scattered light, respectively, λ is the wave length of incident light in vacuum, and θ_s is the scattering angle (90° in these experiments). For the situation at hand, $\lambda = 5145$ Å, $n_a = 1.679$, and $n_c = 1.693$ at 5145 Å and room temperature.[7] Elastic constants can be calculated from

$$c = \rho v^2 ,$$

in which ρ is the crystal density ($\rho = 1.256$ g/cm³ at $T = 300$ K).[10] As interest resides in the anomalous behavior of the elastic constants near the phase transition temperature and not their absolute value, temperature dependences of these other (n, ρ, etc.) constants for benzil can be neglected.

Elastic constants for the two soft modes have been calculated and results near the transition are shown in Fig. 4. Within +10K of the transition temperature, a linear dependence approximately holds for the elastic constants as a function of temperature. Thus,

$$c \simeq c^0(T - T_0) ;$$

for the c-axis mode

$$c \simeq 3.8 \times 10^7 \ N/m^2 \deg \ (T_0 = 70 \pm 1 \ \text{K}),$$

and for the a-axis mode

$$c \simeq 1.7 \times 10^7 \ N/m^2 \deg \ (T_0 = 72 \pm 1 \ \text{K}).$$

Elastic constants for the longitudinal phonon along the a axis were also calculated near the transition temperature and the results are depicted in Fig. 5. Anisotropy of phonon frequencies in the $a-c$ plane was measured and the room temperature results are given in Fig. 6. These results are close to those calculated previously.[7]

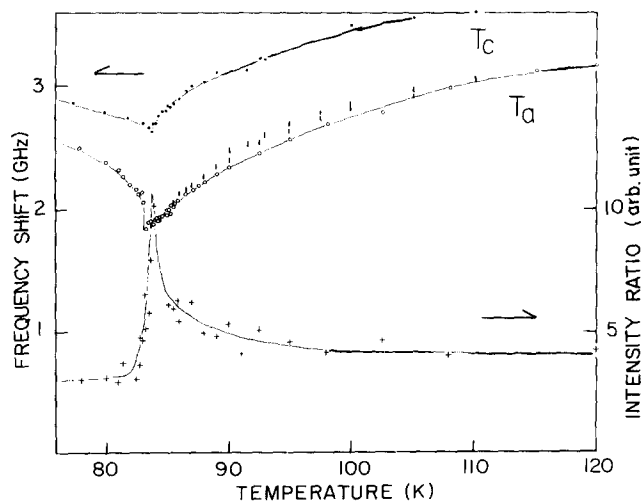Finally, there is a weak (10%–15%) anomaly in c_{66}.

FIG. 3. Temperature dependence of the two transverse (a and c axis) soft mode frequencies (T_a and T_c) and the ratio of the soft mode intensity along the a axis to Rayleigh peak intensity. Two results are given for the a axis mode obtained with two different samples. Measurements on one of these have been taken twice. I_B/I_R and T_a data are for the same crystal and run. Note that the difference in transition temperature for T_c and T_a is due to variation in transition temperature with different samples ($|\Delta T_c| \leq 1$ K for all samples studied).
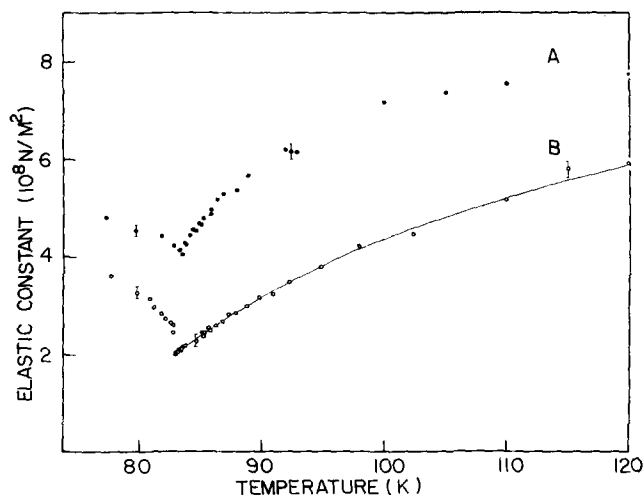
FIG. 4. Temperature dependence of the elastic constants obtained from results shown in Fig. 3. The elastic constants are

(A) c_{44} and (B) $\frac{1}{2}[(c_{66}+c_{44}) - \sqrt{(c_{66}-c_{44})^2 + 4c_{14}^2}]$

for T_c and T_a, respectively. Full line is calculated by Eq. (21) given in the text. c_{44} softening causes both temperature dependences.

The observed c_{66} begins to deviate from that predicted by the high temperature slope at ~120 K; c_{66} (300 K) ~3×10⁹ N/m^2, c_{66} (83.5 K)~4×10⁹ N/m^2, and the projected value of c_{66} is close to 4.8×10⁹ N/m^2. This softening of c_{66} renders it roughly temperature independent near the transition region.

IV. DISCUSSION

Elastic constant matrices for both phases are given in Table I; notation of Ref. 7 has been followed. Correspondence between elastic constants in the high and low temperature phases is given in Table II. Trans-
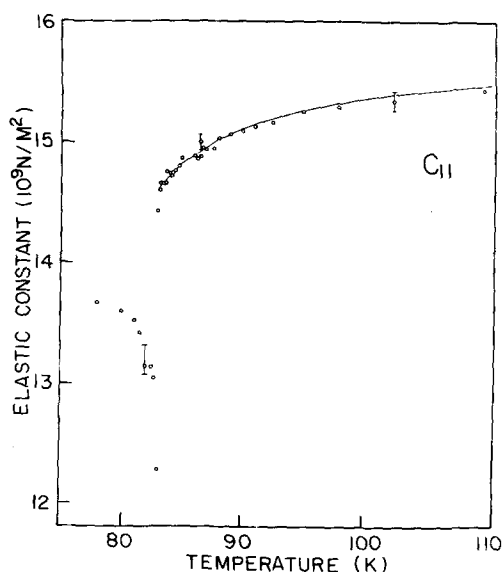

FIG. 6. Anisotropy of Brillouin shifts in the a–c plane at room temperature. A doubly degenerated pure transverse mode propagating along the c axis splits into two quasitransverse modes. These two modes do not cross in the a–c plane. Previous slowness results given in Ref. 7 can be compared by taking the inverse of the present values.

verse phonon frequencies along the c and a axes are given as

$$\omega_T^2 = c_{44}q^2, \quad c \text{ axis }, \tag{1}$$

and

$$\omega_T^2 = \frac{1}{2}\{(c_{66}+c_{44}) \pm [(c_{66}-c_{44})^2 + 4c_{14}^2]^{1/2}\}q^2, a \text{ axis }. \tag{2}$$

The data reveal that $\omega_T^2 = c_{44}q^2$ behaves as a soft mode. Assuming c_{44} has the strongest temperature dependence, the lower frequency for the a axis can be approximated near the transition temperature for the case $c_{66} \gg c_{44}$ as follows:

$$\omega_T^2 \approx \frac{1}{2}\left[(c_{66}+c_{44}) - \left(c_{66}-c_{44}+2\frac{c_{14}^2}{c_{66}}\right)\right]q^2 = \left[c_{44} - \frac{c_{14}^2}{c_{66}}\right]q^2 . \tag{3}$$

FIG. 5. Temperature dependence of the elastic constant c_{11} near the transition temperature. The full line was calculated by Eq. (21) given in the text.
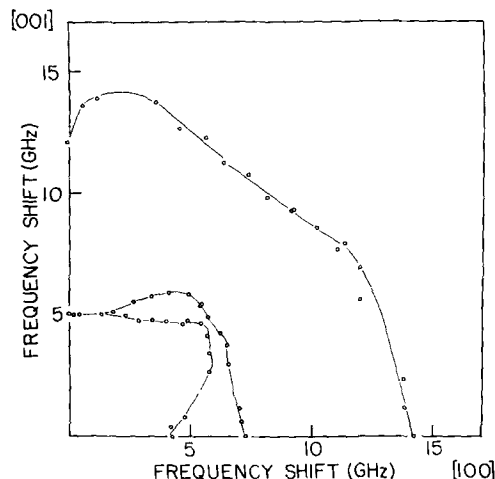
TABLE I. Elastic constant matrices for benzil.

Trigonal phase (D_3^4)					
c_{11}	c_{12}	c_{13}	c_{14}	0	0
c_{12}	c_{11}	c_{13}	$-c_{14}$	0	0
c_{13}	c_{13}	c_{33}	0	0	0
c_{14}	$-c_{14}$	0	c_{44}	0	0
0	0	0	0	c_{44}	$-c_{14}$
0	0	0	0	$-c_{14}$	c_{66}

Monoclinic phase (C_2)					
c_{11}	c_{12}	c_{13}	c_{14}	0	0
c_{12}	c_{22}	c_{23}	c_{24}	0	0
c_{13}	c_{23}	c_{33}	c_{34}	0	0
c_{14}	c_{24}	c_{34}	c_{44}	0	0
0	0	0	0	c_{55}	c_{56}
0	0	0	0	c_{56}	c_{66}

TABLE II. Correspondence between the elastic constants in the high symmetry and low symmetry phases and the approximate polarization designations of their corresponding acoustic phonon modes.

D_3^4	C_2
c_{11} (L)	c_{11} (L)
c_{33} (L)	$\frac{1}{2}[(c_{33}+c_{44}) + \sqrt{(c_{33}-c_{44})^2 + 4c_{34}^2}]$ (QL)
c_{44} (T)	c_{55} (T)
c_{44} (T)	$\frac{1}{2}[(c_{33}+c_{44}) - \sqrt{(c_{33}-c_{44})^2 + 4c_{34}^2}]$ (QT)
$\frac{1}{2}[(c_{44}+c_{66}) \pm \sqrt{(c_{66}-c_{44})^2 + 4c_{14}^2}]$ (QT)	$\frac{1}{2}[(c_{55}+c_{66}) \pm \sqrt{(c_{55}-c_{66})^2 + 4c_{56}^2}]$ (QT)

The form of Eq. (3) gives $T_0 \to T_0 + (c_{14}^2/c_{66}c^0)$ in c_{44} $= c^0(T - T_0)$ and thus this mode can be expected to soften faster than $c_{44}q^2$ alone. In this manner, the two soft transverse modes can share a common origin of instability (the elastic constant c_{44}). Moreover, the lowest phonon frequency propagating along the b axis can be approximated near the transition as

$$\omega_T^2 \approx \left(c_{44} - \frac{c_{14}^2}{c_{11}}\right) q^2 \quad . \tag{4}$$

Therefore, the b-axis transverse mode behaves much like the a-axis mode and the softening of this branch has not been extensively investigated. Since $c_{11} > c_{66} = \frac{1}{2}(c_{11} - c_{12})$, the a-axis mode softens faster than the others.

As we have pointed out in the Introduction, benzil is piezoelectric even in the high temperature phase and thus the dielectric and elastic properties cannot be rigorously separated. Following the theory of piezoelectricity,[13] the free energy of a crystal may be expanded in terms of effective dielectric and elastic constants as

$$F = \frac{1}{2} \chi^0 P^2 - aPe + \frac{1}{2} c^0 e^2 \tag{5}$$

in which χ^0 = dielectric susceptibility, c^0 = elastic constant, a = piezoelectric constant, P = electric polarization, and e = strain. Using Eq. (5), the external electric field E and the external stress X can be calculated from

$$E = \frac{\partial F}{\partial P} = \frac{P}{\chi^0} - ae \tag{6}$$

and

$$X = \frac{\partial F}{\partial e} = c^0 e - aP \quad . \tag{7}$$

Effective dielectric constants and elastic constants are

then given by

$$\frac{\partial E}{\partial P} = \frac{1}{\chi} = \frac{1}{\chi^0} - \frac{a^2}{c^0} \tag{8}$$

and

$$\frac{\partial X}{\partial e} = c = c^0 - a_0^2 \chi^0 \quad . \tag{9}$$

As discussed earlier, benzil has only a weak dielectric anomaly, even near the transition temperature. Nonetheless, it must be pointed out that experimentally χ and c, and not χ^0 and c^0, are observed for piezoelectrics in the free crystal. It is suggested by the previous discussion, however, that the dielectric contribution to the elastic anomalies can be neglected for benzil. For small dielectric contributions, this neglect results only in a shift of absolute values. In the ensuing discussion only the elastic portion of the benzil phase behavior will be treated. This approximation is equivalent to extending the space group of benzil (D_3) into a higher group like D_{3d} by adding an inversion center.

Raich and Bernstein have previously presented a Landau mean field theory of the phase transition in triazine.[11] Triazine has a crystal structure space group of D_{3d}^5 ($R\bar{3}c$) symmetry and a temperature (pressure) induced phase transition due to a c_{44} elastic constant instability.[17] Under the above approximations this theory can be extended to cover benzil; as D_3 becomes D_{3d}, the E irreducible representation of D_3 becomes equivalent to E_g (second rank tensor basis functions) and E_u (vector basis functions) of irreducible representations of D_{3d}. As in the case of triazine, we introduce doubly degenerate order parameters (Q_1, Q_2) as suggested by recent Raman[6] and infrared[5] spectroscopic results. These order parameters can be considered to be phonon amplitudes. The free energy is given as[11,18]

$$F = F_0 + \frac{a}{2}(Q_1^2 + Q_2^2) + \frac{b}{3}Q_1(Q_1^2 - 3Q_2^2) + \frac{c}{4}(Q_1^2 + Q_2^2)^2 + \frac{1}{2}\left(\frac{c_{11}^0 + c_{12}^0}{2}\right)(e_1 + e_2)^2 + \frac{1}{2}c_{33}^0 e_3^2 + \frac{1}{2}c_{44}^0(e_4^2 + e_5^2) + \frac{1}{2}c_{66}^0(e_6^2 + e_7^2)$$

$$+ c_{14}^0(e_4 e_7 - e_5 e_6) + A(e_4 Q_1 - e_5 Q_2) + B(e_7 Q_1 + e_6 Q_2) + C\left[e_4\left(\frac{Q_1^2 - Q_2^2}{2}\right) - e_5 Q_1 Q_2\right] + D\left[e_7\left(\frac{Q_1^2 - Q_2^2}{2}\right) + e_6 Q_1 Q_2\right] + \cdots , \tag{10}$$

in which $a = a_0(T - T_0)$, $c_{66}^0 = \frac{1}{2}(c_{11}^0 - c_{12}^0)$, and $e_7 = (e_1 - e_2)$.   Three equivalent domains are predicted:

Domain I:

$$(Q_1 , \quad e_4 , \quad e_7) \ ;$$

Domain II:

$$(-\tfrac{1}{2} Q_1 + \tfrac{1}{2}\sqrt{3}Q_2 \quad , \quad -\tfrac{1}{2} e_4 + \tfrac{1}{2}\sqrt{3}e_5, \quad -\tfrac{1}{2} e_7 + \tfrac{1}{2}\sqrt{3}e_6) \ ;$$

Domain III:

$$(-\tfrac{1}{2} Q_1 - \tfrac{1}{2}\sqrt{3}Q_2 , \quad -\tfrac{1}{2} e_4 - \tfrac{1}{2}\sqrt{3}e_5 \quad , \quad -\tfrac{1}{2} e_7 - \tfrac{1}{2}\sqrt{3}e_6) \ .$$

Considering domain I alone, the free energy can be more simply described as

$$F = F_0 + \tfrac{1}{2} aQ_1^2 + \tfrac{1}{3} bQ_1^3 + \tfrac{1}{4} cQ_1^4 + \tfrac{1}{2} c_{11}^0 e_1^2 + \tfrac{1}{2} c_{44}^0 e_4^2 + c_{14}^0 e_1 e_4$$
$$+ AQ_1 e_4 + BQ_1 e_1 + \tfrac{1}{2} CQ_1^2 e_4 + \tfrac{1}{2} DQ_1^2 e_1 \ . \qquad (11)$$

This approach yields temperature dependent effective elastic constants by expanding them in powers of the strain e_5 (our e_4) near the phase transition temperature. As we are interested not only in soft mode behavior but also discontinuities at T_c, another method[19] will be employed. Both phases can be treated simultaneously by introducing spontaneous values and fluctuations around these values for Q_1, e_1, and e_4. Three equations are thereby generated:

$$(\partial F/\partial Q_1) = (a + bQ_1 + cQ_1^2)Q_1 + (A + CQ_1)e_4 + (B + DQ_1)e_1$$

$$= \mathcal{E}_1 \ , \qquad (12)$$

$$(\partial F/\partial e_1) = c_{11}^0 e_1 + (B + \tfrac{1}{2} DQ_1)Q_1 = X_1 \ , \qquad (13)$$

$$(\partial F/\partial e_4) = c_{44}^0 e_4 + (A + \tfrac{1}{2} CQ_1)Q_1 = X_4 \ , \qquad (14)$$

in which $\mathcal{E}_1$ is an external field conjugate to the order parameter Q_1 and X_i ($i = 1, 4$) are external stresses. Replacing variables η_i with $\eta_i + \tilde{\eta}_i$ ($\tilde{\eta}_i$ is the fluctuating value of η_i) in Eqs. (12)–(14), the lowest order terms determine a set of equations which generate spontaneous values of the variables and have exactly the same form as Eqs. (12)–(14) with zero spontaneous values of the external fields. Linearized relations between fluctuations and fields can then be employed to generate susceptibilities

$$(a' + 2bQ_1 + 3cQ_1^2)\tilde{Q}_1 + (A + CQ_1)\tilde{e}_4 + (B + DQ_1)\tilde{e}_1 = \tilde{\mathcal{E}}_1 \ ,$$

$$c_{11}^0 \tilde{e}_1 + (B + DQ_1)\tilde{Q}_1 = \tilde{X}_1 \ , \qquad (15)$$

$$c_{44}^0 \tilde{e}_4 + (A + CQ_1)\tilde{Q}_1 = \tilde{X}_4 \ ,$$

in which $a' = a + Ce_4 + De_1$. There are, of course, higher order terms in fluctuations which can make contributions to Eq. (15) even in the high temperature phase. Landau theory neglects such contributions, some of which will be discussed below.

Effective elastic constants can be obtained from Eq. (15) and are defined as follows:

For the L mode with $\tilde{\mathcal{E}}_1 = \tilde{e}_4 = 0$ and $\tilde{X}_1 \neq 0$,

$$c_{11} = \frac{\partial \tilde{X}_1}{\partial \tilde{e}_1} = c_{11}^0 - \frac{(B + DQ_1)^2}{a' + 2bQ_1 + 3cQ_1^2} \ . \qquad (16)$$

For the T mode with $\tilde{\mathcal{E}}_1 = \tilde{e}_1 = 0$ and $\tilde{X}_4 \neq 0$,

$$c_{44} = \frac{\partial \tilde{X}_4}{\partial \tilde{e}_4} = c_{44}^0 - \frac{(A + CQ_1)^2}{a' + 2bQ_1 + 3cQ_1^2} \ . \qquad (17)$$

The above constraints used to derive the elastic constants insure that $(\partial e_4/\partial e_1) = (\partial e_1/\partial e_4) = 0$ for these linearized equations. Treating $\tilde{X}_1$ and $\tilde{X}_4$ like $\mathcal{E}_1$ is inappropriate in this instance because two strain variables are required.

In the high temperature phase, $Q_1 = e_1 = e_4 = 0$ and the above two expressions can be simplified considerably

$$c_{11} = c_{11}^0 - \frac{B^2}{a} \ , \qquad T > T_c \ , \qquad (18)$$

$$c_{44} = c_{44}^0 - \frac{A^2}{a} \ , \qquad T > T_c \ . \qquad (19)$$

Using Eq. (3), effective a-axis elastic constants for the high temperature phase are

$$c_T = c_{44} - \frac{c_{14}^2}{c_{66}} \approx c_{44} - \frac{(c_{14}^0)^2}{c_{66}^0} = \left[c_{44}^0 - \frac{(c_{14}^0)^2}{c_{66}^0} \right] - \frac{A^2}{a} \ . \qquad (20)$$

These three equations can be put into the following form:

$$c_{\text{eff}} = c^0 \frac{T - T_2}{T - T_1} \ . \qquad (21)$$

With data shown in Figs. 4 and 5, parameters appearing in Eq. (21) are determined for longitudinal and transverse modes as

$$c_L = 1.58 \frac{T - 73.4}{T - 72.6} (10^{10} \ \text{N/m}^2) \ , \qquad (22)$$

$$c_T = 0.107 \frac{T - 74.4}{T - 37.2} (10^{10} \ \text{N/m}^2) \ . \qquad (23)$$

In these two equations, it has been assumed that temperature dependence of c^0 within the narrow temperature range around T_c can be neglected. These equations are also plotted in Figs. 4 and 5. Numerical estimates of constants appearing in the free energy expression Eq. (10) can be calculated using Eqs. (20) and (23)

$$\frac{A^2}{a_0} = 3.98 \times 10^{10} \ (\text{N/m}^2 \text{deg}) \ ,$$

$$T_1 = T_0 = 37.2 \ \text{K}, \quad T_c = 83.5 \ \text{K} \ ,$$

and

$$\left[c_{44}^0 - \frac{(c_{14}^0)^2}{c_{66}^0} \right] \sim 0.11 \times 10^{10} \ (\text{N/m}^2) \ .$$

The last result can be directly compared to experimental results given in Refs. 7 and 20

$$\left(c_{44} - \frac{c_{14}^2}{c_{66}} \right) \sim 0.1 \times 10^{10} \ (\text{N/m}^2) \ \text{at} \ T = 300 \ \text{K} \ .$$

The agreement between our calculated estimate and the experimental value is certainly reasonable considering our estimate is obtained near the transition temperature and that $[c_{44}^0 - (c_{14}^0)^2/c_{66}^0]$ has a weak temperature dependence.

An additional comparison can be made for T_0 with the value obtained by setting the Raman frequency for the E mode in the high temperature phase equal to $\partial^2 F/\partial Q_1^2 = \partial^2 F/\partial Q_2^2 = a = a_0(T - T_0)$. A rough fit of the Raman data yields $T_0 \cong 5$ K. For this case, a best fit for both modes yields $T_{2T} \approx 72.5 \pm 0.5$ K and $c_T^0 = 1.53$ (± 0.03) $\times 10^9$ (N/m^2); and $T_{2L} = 18 \pm 2$ K and $c_L^0 = 1.78$ (± 0.05) $\times 10^{10}$ (N/m^2). Neither of these fits is particularly good; however, again the transverse modes are much better than the longitudinal one.

Thus, the transverse elastic anomalies observed for benzil can be explained by a Landau theory with bilinear strain-order parameter coupling terms. Since the phase transition is first order due to cubic invariants in the free energy expansion, the elastic constants may well, in general, evidence discontinuities at the transition temperature. The small step observed in the transverse mode frequency along the a axis can therefore be understood (Fig. 3).

However, the a-axis longitudinal phonon anomaly cannot be explained with only bilinear coupling with the order parameter. The numerically fitted result given by Eq. (22) yields a factor of 2 larger T_0 than that obtained from the c_T results of Eq. (23). The theoretical treatment presented thus far demands that $T_{1T} = T_{1L} = T_0$ [of Eq. (10)] because only bilinear mean field coupling terms have been considered. Higher order terms, including fluctuations, however, contribute to the phenomenological form of Eq. (21). This gives a value of T_1 for the a-axis longitudinal mode much greater than T_0. Moreover, the discontinuity observed in the longitudinal a-axis mode at the transition temperature (Fig. 5) is probably too large to be accounted for in the above mentioned manner. Therefore, the experimental results and theoretical analysis suggest the existence of non-mean field contributions to the a-axis elastic softening.

The a-axis longitudinal mode discontinuity is similar to that observed in improper ferroelectrics like $Gd_2(MoO_4)_3$[21] and $(NH_4)_2SO_4$.[22] Such anomalies may be understood through higher order coupling terms between the order parameters and strains as given in Eq. (10) by $\frac{1}{2} De_1 Q_1^2$, etc. Terms of this nature are referred to as electrostriction and anomalies associated with these higher order couplings have been considered previously.[23] Following Rehwald,[24] the elastic anomaly due to this interaction is found to be

$$\Delta c_{11} = \frac{1}{k_B T} \frac{D^2}{4} \left(4 Q_1^2 \langle |\bar{Q}_1|^2 \rangle + \langle |\bar{Q}_1|^2 |\bar{Q}_1|^2 \rangle \right) . \tag{24}$$

The first term in Eq. (24) vanishes in the high temperature phase and is already included in Eq. (16). For a second-order transition $\langle |\bar{Q}_1|^2 \rangle \sim -Q_1^2$ and this term always gives a step to lower elastic constant values at T_c. Thus, for benzil this term will contribute to the sharp decrease in c_{11} at the transition point and will also be responsible for a weak temperature dependence below the transition temperature. The second term in Eq. (24) survives even in the high temperature phase and contributes to general mode softening, depending on the order parameter susceptibilitiy and the specific heat due to order parameter fluctuations.[24] Therefore, the elastic anomaly in the longitudinal mode near the transition temperature can consist of two terms

$$c_{11} = c_{11}^0 - \frac{(B + DQ_1)^2}{a' + 2bQ_1 + 3cQ_1^2} - \frac{1}{k_B T} \frac{D^2}{4} \langle |\bar{Q}_1|^2 |\bar{Q}_1|^2 \rangle. \tag{25}$$

This may be written as

$$c_{11} = c_{11}^0 - \frac{(B + DQ_1)^2}{a' + 2bQ_1 + 3cQ_1^2} - \Lambda \pm \left| \frac{T - T_0}{T_0} \right|^{-\rho \pm} , \tag{26}$$

in which the $\pm$ signs refer to the high and low temperature phases, respectively.

This expression can account for the c_{11} (soft L_a mode) behavior in a qualitative fashion. In the high temperature phase, Eq. (21) should be replaced in the data analysis, therefore, with

$$c_{11} = c_{11}^0 \left[\frac{T - \left(T_0 + \frac{B^2}{a_0 c_{11}^0} \right)}{T - T_0} \right] - \Lambda + \left| \frac{T - T_0}{T_0} \right|^{-\rho +} . \tag{27}$$

Numerical fitting using Eq. (27) with $T_0 = 37.2$ K and a temperature dependent c_{11}^0 has been repeated with little success. In order to get a reasonable fit, T_0 must approach 80 K in Eq. (27). More will be presented on this issue shortly.

As a further application of the Landau mean field theory to the benzil phase transition, phonon frequency anisotropy in the $a-c$ plane at room temperature was calculated using the full dynamical matrix. Results are shown in Fig. 7 and should be compared with Fig. 6.

Ultrasonic experiments at room temperature[20] give lower sound velocity values (by about 3%–5%) than those obtained from Brillouin scattering.[7,25] The difference in these velocities is outside the contribution from dispersion effects, which are expected to be of the order of less than 1%. This suggests the possibility that some relaxation process is involved with the dynamical behavior of benzil. From the standpoint of a ferroelectric phase transition, the anomaly at 84 K in benzil can be regarded as an order–disorder transition of the permanent dipole moments of the individual molecules. One possible mechanism for such a relaxation effect would be a dipolar orientation–relaxation process. Thereby, the anomaly in the intensity ratio of Brillouin soft mode scattering to Rayleigh scattering shown in Fig. 3 might be explained by a critical slowing down of some (dipolar) relaxation time. This relaxation time is consistent with the generalized Lyddane–Sachs–Teller relaxation[26] given by

$$\frac{\epsilon_0}{\epsilon_\infty} = \frac{\tau_L}{\tau_T} \Pi \frac{\omega_L^2}{\omega_T^2} , \tag{28}$$

in which τ_T is the (critical) transverse relaxation time and τ_L is the (usually assumed noncritical) longitudinal relaxation time. In order that the observed small dielectric anomaly be maintained by this equation,

$$\omega_L \sim \omega_T \sim (T - T_0)$$

and

$$\tau_L \sim \tau_T \sim (T - T_0)^{-1} .$$

Thus, ultrasonic and dielectric dispersion measurements near the transition point will yield important dynamical information for the benzil phase transition. Clearly, the concept of some relaxation process affecting the frequency dispersion is consistent with the existing benzil data.

Finally, previous x-ray results on benzil at 74 K[3] and their proposed incorporation into a theory of the benzil phase transition[8] should be discussed. Toledano has developed a theory for the benzil phase transition based on the observed doubling of translational symmetry in the (0001) plane of the hexagonal unit cell. Cell doubling was accounted for by introducing zone boundary
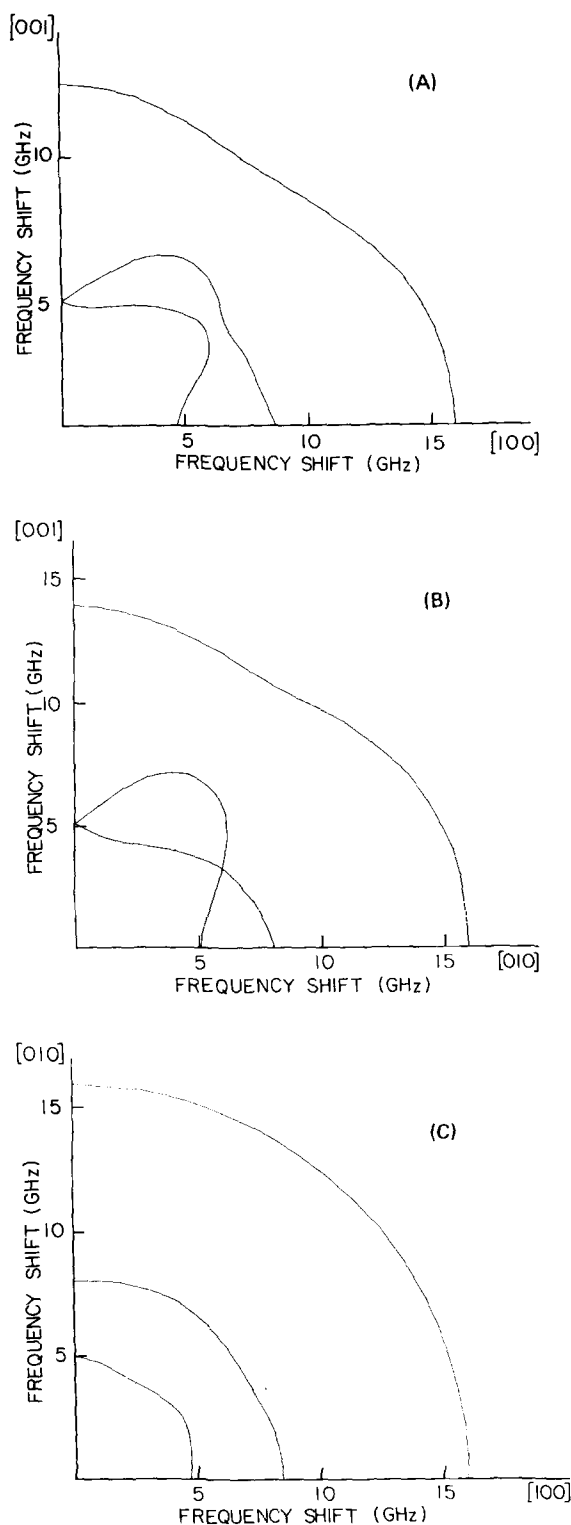
FIG. 7. Theoretical calculations of the Brillouin shift anisotropy for benzil at room temperature: (A) (ac plane), (B) (bc plane), and (C) (ab plane).

order parameters at the M point in the hexagonal Brillouin zone. The star associated with this representation of the translation group has three components and thus the order parameter is three dimensional. These order parameters couple to the E zone center order parameters introduced in the above discussion. This

theory assumes that the zone center instability triggers the zone boundary instability through anharmonic interaction given by

$$F_{\text{int}} = \delta[Q_1(2\zeta_1^2 - \zeta_2^2 - \zeta_3^2) + Q_2\sqrt{3}(\zeta_2^2 - \zeta_3^2)] \quad , \tag{29}$$

in which (Q_1, Q_2) are again the zone center E order parameters and $(\zeta_1, \zeta_2, \zeta_3)$ describe the zone boundary instability. As a consequence, three phases are predicted:

Phase I: trigonal high temperature phase $(Q = \zeta = 0)$;

Phase II: monoclinic $C2$ with same translation symmetry as phase I $(Q_i \neq 0, \ \zeta = 0)$;

Phase III: monoclinic $C2$ with different translational symmetry from phase I $(Q_i \neq 0, \ \zeta_i \neq 0)$.

Conditions have been presented for a phase I → phase III transition without the appearance of phase II. The free energy associated with the coupling between zone boundary order parameters and strains is given by

$$F_{\zeta-e} = l[\sqrt{3}e_5(\zeta_2^2 - \zeta_3^2) + e_4(2\zeta_1^2 - \zeta_2^2 - \zeta_3^2)] + m[\sqrt{3}e_6(\zeta_2^2 - \zeta_3^2)$$
$$+ e_7(2\zeta_1^2 - \zeta_2^2 - \zeta_3^3)] + n[(e_1 + e_2)(\zeta_1^2 + \zeta_2^2 + \zeta_3^2)] + \cdots . \tag{30}$$

As is easily seen, the postulated zone boundary order parameter contributions to the free energy are of the same form as those arising from higher order fluctuations of the zone center couplings [compare Eqs. (24)–(27)]. Therefore, elastic anomalies expected from this mechanism are of exactly the same form as given by Eq. (24). As mentioned before, in order to obtain a numerical fit for the a-axis longitudinal mode, a more complicated expression than that given in Eq. (26) is required. Such a new equation might have the form of Eq. (26) with the added term

$$-\Delta_+ \left| \frac{T - T_M}{T_M} \right|^{-\theta_+} \quad ,$$

which expresses a possible zone boundary mode fluctuation contribution to the softening of c_{11}. Clearly such a total equation has too many parameters to be fit meaningfully to the present experimental results. Unfortunately, elastic measurements cannot separate two superimposed anomalies due to these two electrostrictive-type interactions.

Presently only one experiment[3] has suggested that the translational symmetry is broken at the transition point. This x-ray study reports temperature dependence of the zone center order parameter only. In addition, Brillouin data taken to 35 K evidence no further anomalous behavior in any of the acoustic phonon modes, even though x-ray and infrared studies show an additional discontinuity at ~55 K. Clearly, more precise structural studies and measurements of Bragg point intensities corresponding to zone boundary points (the M point in particular) would be of considerable importance and interest.

V. CONCLUSION

The structural phase transition in benzil at 83.5 K has been investigated using Brillouin scattering from phonons propagating along the a and c axes. Our observations are summarized as follows:

(1) Two transverse modes propagating along the a and c axes behave as soft modes. The related elastic constants are $\frac{1}{2}[(c_{66}+c_{44})-\sqrt{(c_{66}-c_{44})^2+4c_{14}^2}]$ and c_{44}, respectively.

(2) A longitudinal phonon propagating along the a axis is temperature sensitive near the transition point; a λ-type anomaly is observed for this mode.

(3) A longitudinal phonon propagating along the c axis shows no anomaly around the transition temperature as predicted by the triazine Landau theory.

(4) The ratio of the soft mode intensity to Rayleigh peak intensity along the a axis was examined. It was found that this ratio has a maximum at T_c+1 K, which indicates a rapid increasing in the Rayleigh intensity in the high temperature phase.

(5) Anisotropy of phonon frequencies in the $a-c$ plane was determined at room temperature.

These results are analyzed by a mean field Landau theory. Observed elastic constant temperature dependences could be fitted by a relation of the form

$$c = c^0(T - T_2)/(T - T_1) \ .$$

Along the a axis in the high temperature phase c_T^0 $=0.107\times10^{10}$ N/m^2, $T_2=74.4$ K, and $T_1=T_0=37.2$ K and $c_L^0=1.58\times10^{10}$ N/m^2, $T_2=73.4$ K, and $T_1=72.6$ K.

Bilinear coupling constants appearing in the theory could be estimated from the data. To discuss the λ-type anomaly in c_{11}, an electrostrictive-type interaction was introduced. This term also contributes to the elastic softening in the high temperature phase. The effect of a Brillouin zone boundary instability on the elastic constants was examined and it was found to give contributions similar to those for the electrostrictive interactions from zone center order parameters. A quantitative decomposition of these two contributions must await a more complete and more accurate data set.

Anisotropy in phonon frequencies was calculated based on the triazine theory[27] and good agreement between theoretical and experimental results obtained.

Finally, a possibility of some (dipolar) relaxation process was explored to explain sound velocity dispersion, Rayleigh intensity, and the dielectric anomaly in benzil. Rayleigh correlation measurements are now in progress to obtain more information on this relaxation phenomenon.

[1]P. Esterick and B. E. Kohler, J. Chem. Phys. 59, 6681 (1973).

[2]Y. I. Chan and B. A. Heath, Chem. Phys. Lett. 46, 164 (1977).

[3]G. Odou, M. Mone, and V. Warin, Acta Crystallogr. Sect. A 34, 459 (1978).

[4]A. Dworkin and A. Fuchs, J. Chem. Phys. 67, 1789 (1977).

[5]B. Wyncke, F. Brehat, and A. Hadni, Ferroelectrics 25, 617 (1980).

[6]J. Sapriel, A. Boudou, and A. Perigand, Phys. Rev. B 19, 1484 (1979).

[7]R. Vacher, M. Boissier, and J. Sapriel, Phys. Rev. B 23, 215 (1981).

[8]J. C. Toledano, Phys. Rev. B 20, 1147 (1979).

[9]K. Higashi, Bull. Chem. Soc. Jpn. 13, 158 (1938).

[10]C. J. Brown and R. Sadanaga, Acta Crystallogr. 18, 158 (1965).

[11]J. C. Raich and E. R. Bernstein, J. Chem. Phys. 73, 1955 (1981).

[12]I. U. Heilman, W. D. Ellenson, and J. Eckert, J. Phys. C 12, L185 (1979).

[13]F. Jona and G. Shirane, Ferroelectric Crystals (Pergamon, New York, 1962).

[14]H. Klapper, J. Cryst. Growth 10, 13 (1971).

[15]R. Vacher and L. Boyer, Phys. Rev. B 6, 639 (1972).

[16]V. Chandrasekhran, Proc. Indian Acad. Sci. Sect. A 33, 183 (1951).

[17]References cited in Ref. 11.

[18]The axes are rotated for benzil with respect to triazine to conform with the more standard notation which gives the elastic constant matrix presented in Table I. Triazine axes were chosen to allow y (actually R_y) to coincide with the C—H bond and the crystallographic b axis. (See Fig. 1 of Ref. 11 and compare the elastic matrices given here in Table I and in Appendix A of Ref. 11.)

[19]R. Blinc and B. Zeks, Soft Modes in Ferroelectrics and Antiferroelectrics (Elsevier, New York, 1974).

[20]S. Haussuhl, Acta Crystallogr. 23, 666 (1967).

[21]L. E. Cross, A. Fouskova, and S. E. Cummins, Phys. Rev. Lett. 21, 812 (1968)—resonance method; S.-I. Itoh and T. Nakamura, Phys. Lett. A 44, 461 (1973)—Brillouin scattering.

[22]T. Ikeda, K. Fujibayashi, T. Nagai, and J. Kobauashi, Phys. Status Solidi 16, 279 (1973)—resonance method; A. Yoshihara, T. Fujimura, and K.-I. Kamiyoshi, J. Phys. Soc. Jpn. 44, 1241 (1978)—Brillouin scattering.

[23]For example, see T. Schwabl, Phys. Rev. B 7, 2038 (1973); V. Dvorak, Czech. J. Phys. B 21, 836 (1971).

[24]W. Rehwald, Adv. Phys. 22, 721 (1973).

[25]D. A. Dows and S. R. Chiang, in Proceedings of the 21st European Congress on Molecular Spectroscopy, Strasbourg, France, 1975.

[26]A. S. Chaves and S. P. S. Porto, Solid State Commun. 13, 865 (1973).

[27]J. C. Raich, E. R. Bernstein, and A. Yoshihara, Chem. Phys. Lett. 82, 138 (1981).